

Chemical Modification of Controlled-Pore Silica with *N*-Propylsalicylaldimine

Khaled Abou-El-Sherbini,¹ I. M. M. Kenawy,² R. M. Issa³

¹*Inorganic Chemistry Department, National Research Centre, Dokki, Cairo, Egypt*

²*Department of Chemistry, Faculty of Science, Mansoura University, Mansoura, Egypt*

³*Department of Chemistry, Faculty of Science, Tanta University, Egypt*

Received 5 October 2001; accepted 9 September 2002

ABSTRACT: Two controlled-pore silica phases were prepared with a sol-gel precursor from a sodium silicate solution. *N*-Propylsalicylaldimine was immobilized on these silica species to be used as chelating ion exchangers (IE11 and IE2). The monomer phase was also prepared for comparison. The *N*-propylsalicylaldimine moiety was detected by Fourier transform infrared and ultraviolet in both the ion exchangers and the monomer phases. ¹H-NMR and mass spectrometry of the monomer also confirmed the structure. The capacity (*C*) of the ion exchangers was dependent on the porosity of the ion exchanger ($C_{IE11} = 0.36$ mmol of Cu/g

and $C_{IE2} = 0.026$ mmol of Cu/g). The uptake behavior of IE11 toward some metal ions was studied, and log distribution coefficient (k_d) was within the range of 2.19–5.16. Also, thermogravimetric and differential thermogravimetric analysis data were used to study the kinetics of the thermal decomposition process of IE11. Some thermodynamic parameters for the ion exchanger were calculated by the application of the rate theory of the first-order reaction. © 2003 Wiley Periodicals, Inc. *J Appl Polym Sci* 88: 3159–3167, 2003

Key words: modification; silicas; ion exchangers

INTRODUCTION

Because of the low concentration of heavy metal ions and possible matrix interference, separation and preconcentration are prerequisites for determination. Various methods, such as electrodeposition, coprecipitation, solvent extraction, evaporation, and freeze drying, can be used before determination.^{1–7} Among the different separation techniques, the chelating ion exchange method is advantageous because the sorbent (ion exchanger) is totally insoluble and inert to the solution. Also, the ion exchange method has a low risk of contamination. Many common chelating ligands have been immobilized on different supports to be used as chelating ion exchangers. 8-Hydroxyquinoline has been immobilized on polymeric vinyl solid supports,⁸ spherical cellulose,⁹ and fluorinated metal alkoxide glass (MAF-8HQ).¹⁰ Pyridylazo- β -naphthol (PAN) has been bonded to chemically modified chloromethylated polystyrene.¹¹ Izatt et al.¹² enriched traces of Ag⁺ and Hg²⁺ by the retention of their ions on silica-gel-bound diazo-18-crown-6,3.

Silica has attracted particular interest as an important alternative support for the immobilization of chelating agents because it is commercially available, has good mechanical stability, and is less susceptible than

organic polymers to microbial and nuclear degradation, shrinking, and swelling.^{13,14} However, silica has two serious disadvantages. First, it is susceptible to hydrolysis at pH higher than 10, and so the working range is limited to lower pH values. Second, it has a small surface area, which yields a lower capacity. For the surface area to be enlarged, either silica gel or controlled-pore silica is used.

Although the Schiff bases are known to be easily prepared chelating ligands and are well characterized, little interest has been given to their immobilization on polymers to be used as ion exchangers. The aim of this study was to synthesize silica-based ion exchanger functionalized with a Schiff base to be used in the separation and preconcentration of heavy metals.

EXPERIMENTAL

Instrumentation

An analysis of Cd(II), Cu(II), and Pb(II) was performed with a PerkinElmer 2380 flame atomic absorption spectrophotometer (Vernon Hills, IL).

For X-ray analysis, for structural investigations, a powder diffractometer (Philips PW1730 X-ray generator, Eindhoven, The Netherlands) was used with Cu K α radiation (30 kV, 8 mA).

For thermogravimetric analysis, an automatic recording thermobalance (DuPont 951 instrument, Wilmington, DE) was used in this study. The samples were subjected to heat at a rate of heating of 10°C/min from room temperature to 750°C in N₂.

Correspondence to: I. M. M. Kenawy (kh_sherbini@yahoo.com).

TABLE I
Fraction Analysis of BSG and the Yields After the Leaching of Boron

No.	Particle size (μm)	BSG1 (g)	CPS1 (g)	B ₂ O ₃ (%)	B _(ex) (%)	BSG2 (g)	CPS2 (g)	B ₂ O ₃ (%)	B _(ex) (%)
1	<75	121.9	28.2	9.75	97.1	60	53.9	14.6	43.7
2	112 > 75	81.9	19.4	11.86	96.4	2.2	—	—	—
3	160 > 112	28.6	7.0	14.7	95.4	0.5	—	—	—

B_(ex) = extracted boron.

IR absorption spectra were recorded with a Mattson 5000 Fourier transform infrared (FTIR) spectrometer, Cambridge, UK, for a sample of 2–3 mg diluted with 300 mg of KBr as a tablet pressed under 10 t/cm².

IR reflection spectra were recorded with a Bruker IFS 48 FTIR spectrometer (Ettlingen, Germany) with a gold ball as a reference. The sample, in the form of a fine powder, was flattened on a stainless steel sheet, with a drop of acetone, which was allowed to vaporize, and then the reflectance was measured.

Raman spectra were recorded with a RFS100/s laser, Ettlingen, Germany (1064 nm, power ~ 100–250 mV; IAAC/TU-Berlin). The reference was microcrystalline WO₃.

Ultraviolet (UV) absorption spectrometric measurements were performed with a Unicam ultraviolet-visible UVZ spectrometer (Cambridge, UK), and the samples were introduced as slurry with nujol on Whatman filter paper strips.

¹H-NMR measurements was performed for the monomer of the ion exchanger *N*-propyltrihydroxysilanesalicylaldehyde (SAPHS) in dimethyl sulfoxide (DMSO) with a JEOL 270 EX-spectrometer (Tokyo, Japan).

Mass spectrometry was performed with a Finnigan Mat SSQ 7000 gas chromatography/mass spectrometry mass spectrometer (Herts, UK).

Micrographs were taken with scanning electron microscopy (SEM; QJSM-T20 SEM, JEOL, Tokyo, Japan).

The pH-metric titration measurements were performed with a Metrohm 736 GP Titrino automatic potentiometer (Herisau, Switzerland), and the measurements were recorded with a Metrohm Herisau Brinkmann E536 potentiograph. The ion exchanger (100 mg) was added to 25 cm³ of a 0.02M KCl, 0.002M HCl, and 0.001M metal salt solution and titrated against 0.0075M NaOH at 25°C.

For pH measurements, a Hanna pH meter (Rome, Italy) with an expanded scale was used with an accuracy of ± 0.01 log unit. It was first standardized with 0.05M potassium hydrogen phthalate, yielding pH 4.01 and a tablet of pH 9.2 at 25°C.

Synthesis

Controlled-pore silica

Borosilicate glass (BSG) was prepared by a sol-gel process according to the literature.¹⁵ In this method,

H₃BO₃ (435.48 and 34.84 g) was dissolved in the colloidal SiO₂ sol in ratios of Si/B \cong 1:6.5 and 2:1 to obtain BSG1 and BSG2, respectively; they were then crushed and milled in a ball mill for 4 h, and the resulting powder was sieved. To each fraction, 300 cm³ of 5M HCl was added and refluxed in a water bath for 5 h/day for 2 weeks. The supernatant liquor was daily renewed with fresh HCl so that controlled-pore silicas CPS1 and CPS2, respectively, are obtained. The porous silica was filtered, washed with distilled water, and dried at 90°C for 24 h. The results are shown in Table I.

Ion exchanger

For the grafting of silica, the method described in the literature^{16,17} was followed. γ -Aminopropyltrimethoxysilane (APMS; 36 cm³) was added to 18 g of CPS1₁ or CPS2₁ (the subscript refers to the fraction size number, which was less than 75 μm) suspended in 150 cm³ of xylene, and then the mixture was refluxed in a water bath at 80°C with stirring for 24 h. The yield, 20.0 or 18.5 g (grafted porous silicas GPS1₁ and GPS2₁, respectively), was washed with ethyl alcohol and dried at 80°C. For a silica-based *N*-propylsalicylaldehyde Schiff-base ion exchanger to be obtained, 15 cm³ of salicylaldehyde was refluxed with 11 g of GPS1₁ suspended in 50 cm³ of DMSO in a water bath at 90°C with stirring for 3 h. A bright yellow product was obtained (IE11). The product was washed thoroughly with ethyl alcohol, dried at 80°C for 6 h, and weighed to be 13.5 g. The same process was repeated to obtain 11.4 g of IE2 from GPS2₁.

Monomer phase of the ion exchanger

For the preparation of the monomer phase of the ion exchanger, 20 cm³ of APMS was refluxed with 200 cm³ of distilled water for 72 h at 80°C, and then water was allowed to evaporate to dryness. Five grams of the glassy yellowish product [suggested to be γ -aminopropyltrihydroxysilane (APHS)] was milled into a fine powder and put in a basket filter paper in a Soxhlet condenser. Salicylaldehyde (10 cm³) was added to 150 cm³ of ethyl alcohol in a round-bottom flask connected to the Soxhlet condenser, and then the apparatus was refluxed for 3 weeks. Finally, a deep yellow oily product (suggested to be the Schiff base of salicylaldehyde with

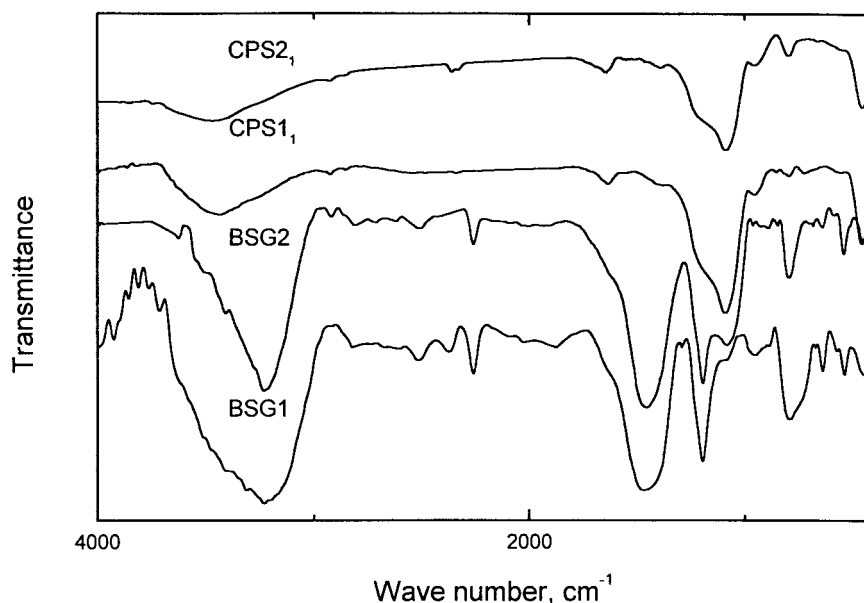


Figure 1 IR absorption spectra of BSG and porous silica yielded after HCl leaching.

APHS, i.e., SAPHS) formed, which was then boiled several times with pure ethyl alcohol and water, dried at 80°C, and kept in desiccator.

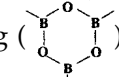
RESULTS AND DISCUSSION

Controlled-pore silica

X-ray diffraction (XRD)

XRD patterns of the BSG samples BSG1 and BSG2 indicated that both samples showed diffractograms of typical amorphous phases, an important indication of the glassy properties of the samples.^{15,18} BSG1 showed high sensitivity toward humidity, as indicated from the detection of diffraction lines at $2\theta = 28.00$ and 14.62° due to H_3BO_3 (sassolite, PDF no. 30-0199) in powdered samples subjected to air for several days. This was expected because of the high content of boron in this glass sample. However, an amorphous hump was observed at $2\theta = 22.4^\circ$, especially in BSG2, which was attributed to amorphous cristoballite, but no lines from any crystalline B_2O_3 or SiO_2 phases were detected.

IR spectra

BSG1 and BSG2 showed band-rich IR absorption patterns (Fig. 1). BSG1 showed IR bands at 457, 644, 718, 796, 1194, 1389, 1496, and 1656 cm^{-1} , which were assignable to the vibration modes of Si—O—Si bending,¹⁹ O—B—O out-of-plane bending,²⁰ B—O—Si bending,^{19,21} symmetric Si—O—Si stretching,²⁰ longitudinal SiO_2 lattice vibration,²⁰ ring stretching vibration of the broxol ring ()¹⁵ stretching of trigonal BO_3 units,¹⁵ and bending of molecular H_2O ,²⁰ re-

spectively. The same bands were observed in BSG2, except for the band assigned to B—O—Si bending, which could not be observed. Also, the band assigned to the ring stretching vibration of the broxol ring decreased.

The IR spectra of BSG1 indicated the presence of B_2O_3 as broxol groups bonded to the SiO_4 lattice network and to each other, whereas in BSG2, these groups decreased as a result of the lower B/Si ratio.

IR absorption spectra of the porous silicas CPS1₁ and PSO2₁ (Fig. 1) showed the disappearance of the peaks assigned to B—O and B—O—Si vibrations at 644, 718, 1389, and 1496 cm^{-1} . This was due to the leaching of boron from the SiO_2 network.

Raman spectra

The Raman spectra of the BSG samples are shown in Figure 2. BSG1 showed two sharp peaks at 499 and 879 cm^{-1} that were assignable to the ring O—B—O in-plane bending (ν_7 , E)²² and the broxol ring vibrations.²³ These peaks were strongly shifted to higher wave numbers than those reported for ternary BSG (475 and 810 cm^{-1} , respectively). Accordingly, a stronger bending within the B—O network may be concluded that could be due to weaker bending to the neighboring Si atoms or more likely to severe hydration from air humidity to H_3BO_3 . These two peaks appeared also in the Raman spectra of BSG2 but with much lower intensity because of the B/Si ratio. The stretching vibration peaks of bonded water appeared at 3166 and 3247 cm^{-1} . BSG1 also showed a small peak at 1166 cm^{-1} that might correspond to the stretching vibration of the nonequivalent oxygen of the SiO_4 group.²² This peak could not be detected in BSG2,

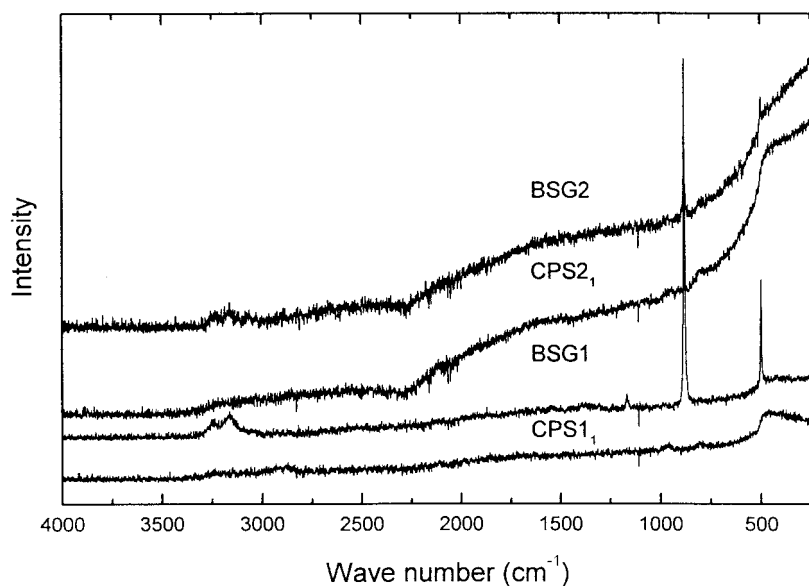


Figure 2 Raman spectra of BSG and controlled-pore silica.

apparently because of the low B/Si ratio leading to fewer B—O—Si bonds. However, these results agreed well with those obtained from IR absorption measurements.

Similar to the IR measurements, the Raman spectra of the porous silicas CPS1₁ and PSO2₁ (Fig. 2) showed the disappearance of all bands previously assigned to the B—O vibrations. Also, a band at 477 cm⁻¹ appeared in both samples and was due to SiO₄ without nonbridging oxygen ions. In general, the Raman spectral patterns of the porous silica samples were characterized by broad and weak peaks, indicating the amorphous structure.

The SEM photos of CPS1₁ and CPS2₁ showed that there were observable differences in the morphology

of the particles: CPS2₁ showed dense and flattened-surface particles with a low surface area, whereas CPS1₁ showed a creased surface with many cavities in the particles and a larger surface area.

Ion exchangers

IR spectra

The IR absorption spectrum of GPS1₁ (Fig. 3) shows three bands at 1100–1200 (broad), 800, and 463 cm⁻¹ assigned to longitudinal SiO₂ lattice vibration,²⁰ symmetric Si—O—Si stretching,²⁰ and Si—O—Si bending,¹⁹ respectively. Weak absorption bands were also

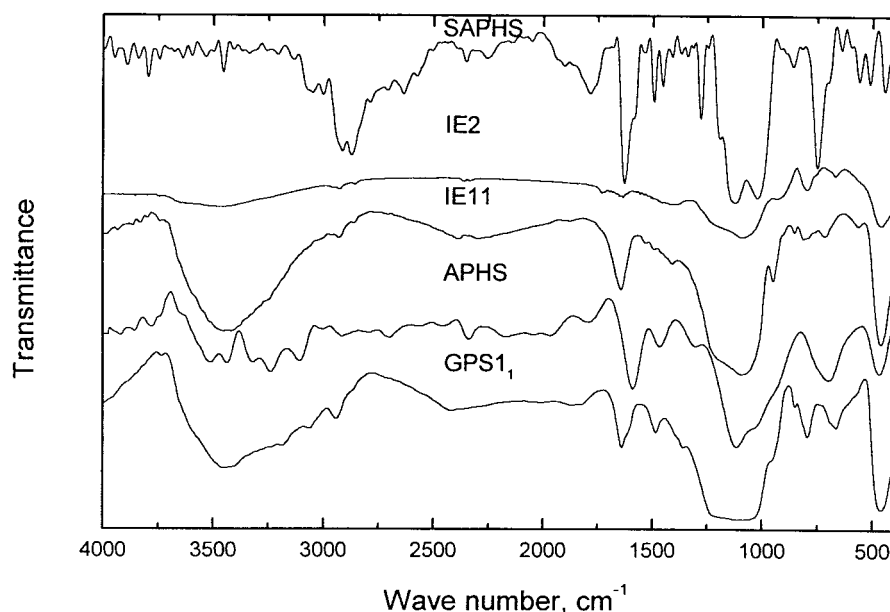
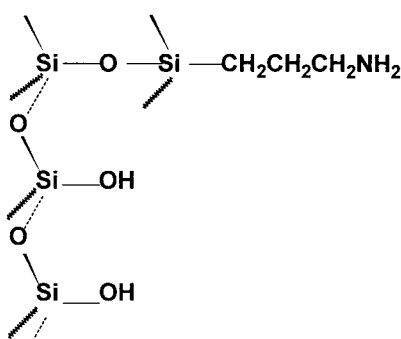


Figure 3 IR absorption spectra of grafted silica and Schiff-base ion exchangers.

observed at 1485 and 2943 cm^{-1} that were assignable to the CH_2 symmetric deformation (δ_s) and asymmetric stretching (ν_{as}) vibrations, respectively.²⁴ The shoulder at 2863 cm^{-1} could be assigned to the symmetric stretching (ν_s) vibration of CH_2 . The absorption band at 3449 cm^{-1} corresponded to $\nu(\text{OH})$. The band at 1640 cm^{-1} may be an overlapped band due to $\delta(\text{OH})$, $\delta(\text{N—H})$ in-plane, and the SiO_2 overtone. The IR absorption bands at 3064 and 3189 cm^{-1} may be attributed to NH_2 (ν_s and ν_{as}). They were strongly shifted to lower wave numbers because of the strong hydrogen bonding with the SiOH groups.²⁴ These two bands were detected in the alike monomer APHS at 3108 and 3240 cm^{-1} , closer to the free amine, which may be attributed to the lower population of the OH groups, as concluded from the lower intensity of the bending vibration band. The shift of the band at 1358 cm^{-1} in the spectrum of GPS1_1 to 1300 cm^{-1} in the that of APHS may be similarly explained, as it was assignable to $\nu(\text{C—N})$. The stronger the hydrogen bonding was between the N—H and the oxygen atoms in the silica lattice, the stronger the C—N bond was and vice versa.

The bands due to the organic constituent could not be detected in GPS2_1 , and this was an indication of the very low content of the organic constituent. The weakness of the bands due to the organic constituent in the IR spectrum of the grafted porous silica in comparison with those from silica was attributed to the fact that organic grafting is a surface phenomenon that depends largely on the surface area of silica. Accordingly, the structure of the grafted silica is suggested to be as shown schematically in the following structure:



The IR absorption spectrum of IE11 (Fig. 3) showed the disappearance of the NH_2 modes of vibrations and the appearance of IR bands related to the organic moiety as weak bands or shoulders in relation to that of silica. A shoulder at 1620 cm^{-1} assigned to the azomethine group [$\delta(\text{C=N})$] and a weak band at 1406 cm^{-1} assigned to $\nu(\text{C—N})$ were detected in the IR spectrum of the ion exchanger.²⁵

The structure suggested from IR was confirmed by the spectrum of the alike monomer SAPHS (Fig. 3), which clearly showed the bands suggested to be due to $\delta(\text{C=N})$ and $\nu(\text{C—N})$ at 1581 and 1406 cm^{-1} , and the

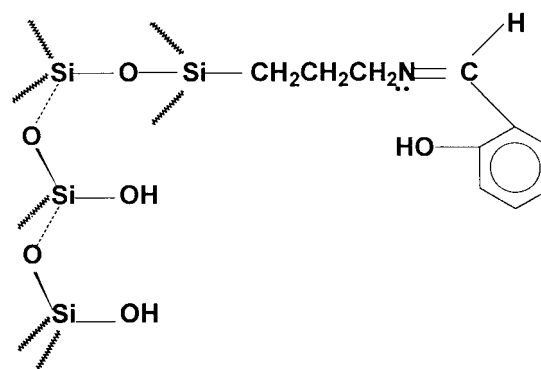
disappearance of the NH_2 modes of vibrations observed in its free amine adduct. The bands due to the SiO_2 vibrations, longitudinal SiO_2 lattice vibration, symmetric Si—O—Si stretching, and Si—O—Si bending appeared also, indicating a partial dehydration polymerization of the trihydroxysilane groups. This can also be concluded from the absence of the OH stretching vibration band.

The phenolic —C=C— vibration band appeared at 1533 cm^{-1} in the absorption spectrum of IE11 and SAPHS. The CH_2 deformation band appeared in the IR spectrum of IE11 as a shoulder at 1453 cm^{-1} , whereas it was a moderate band in that of SAPHS. The weak band at 1492 cm^{-1} , suggested to be due $\delta(\text{N—H})$ in-plane, was yielded from the tautomeric enamine.²⁶

The IR reflection measurement of IE11 (Fig. 4) confirmed the information concluded from the IR absorption spectrum, producing stronger bands from the grafted surface. Moreover, a band was detected at 1276 cm^{-1} assignable to $\delta(\text{O—H})$ in-plane that could not be observed in IR absorption analysis because of the overlapping with the huge band of the longitudinal SiO_2 lattice vibration at 1100–1200 cm^{-1} .

No information could be extracted from IE2 as its organic constituent was much lower because of the smaller surface area. It can be explained that the low B/Si ratio in the parent BSG phase BSG2 (1/2), in comparison with that of BSG1 (6.5/1), led to lower porosity of the yielded controlled-pore silica CPS2_1 than that of CPS1_1 after acid leaching. Moreover, because of the existence of Si—OH groups on the surface, at which the grafting process took place, it was necessary that these groups be accessible by the grafting agent APMS and then salicylaldehyde to form the Schiff base. This requirement was obviously present in CPS1_1 more than CPS2_1 because of the greater presence of the large broxol groups in parent BSG1 than in BSG2. These groups left after acid-leaching pores large enough to accommodate the organic substrate.

The structure of the ion exchangers is suggested to be as follows:



UV measurements

The UV spectrum of IE11 showed the presence of two absorption bands at 314 and 400 nm; this was in good

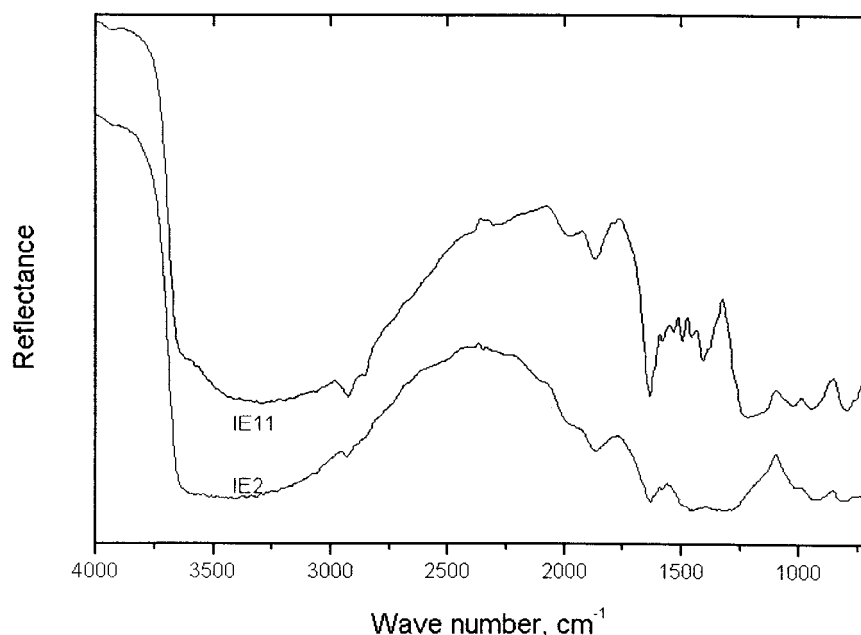


Figure 4 IR reflectance spectra of Schiff-base ion exchangers IE11 and IE2.

agreement with those reported previously for Schiff-base salicylaldimine.²⁷

¹H-NMR and mass spectrometry of the monomer SAPHS

For further confirmation of the structure of the ion exchanger, ¹H-NMR and mass spectrometry were performed on the monomer compound SAPHS, as it was not possible to do these analyses directly on the ion exchanger because it was insoluble. ¹H-NMR of SAPHS dissolved in DMSO showed aromatic protons as multiplets at $\delta = 6.0$ – 7.9 ppm, CH₂—Si at $\delta = 0.5$ ppm, C—CH₂—C at $\delta = 1.5$ ppm, and the last methylene group CH₂—N at $\delta = 3.3$ ppm.²⁴ Phenolic OH disappeared, probably because of the enamine tautomerism. H—C=N— appeared at $\delta = 8.1$ ppm with a broad singlet signal. The three Si—O—H protons appeared in a broad signal (because of hydrogen bonding) at $\delta = 13.4$ ppm.

The mass chromatogram of SAPHS dissolved in ethanol showed the presence of a single peak indicating the purity of the sample. The 100% fragment appeared at $m/e = 143$ and may be due to C₉H₅ON.²⁴

The results obtained from ¹H-NMR and mass spectrometry of SAPHS, which was the monomer of the ion exchanger, were in good agreement with the suggested structure.¹⁰ The presence of the partial polymerization was expected because of the dehydration of the Si—O—H groups.

Thermogravimetry (TG)

The TG curves of IE11 and IE2 are shown in Figure 5. The TG curve of IE11 shows that the ion exchanger

was thermally degraded in two steps. The first stage was attributed to the moisture content (6.1%). The degradation of the organic part of the ion exchanger occurred during the second step between 150 and 480°C. This step was divided into two stages; the first one might have been due to the liberation of the aromatic part. This was confirmed by mass spectrometry of the prepared monomer phase SAPHS, as it showed fission at $m/e = 107$, representing $m + 1$ of Oc1ccccc1. However, mass spectrometry showed a minor fragment at 94 corresponding to $m + 1$ of c1ccc(O)cc1.

During the second part of this stage, the thermal degradation of the organic substrate was extended to approximately 477°C.

According to the weight loss accompanied by the degradation of the organic phase (13.34%), the theoretical capacity of the ion exchanger should have been 0.67 milliequivalent/g.

The TG curve of IE2 similarly showed two degradation stages but with much lower weight loss values attributed to the small surface area with respect to IE11. The first stage was attributed to moisture, whereas the organic degradation stage started at 187°C and finished at 579°C, representing a weight loss of 3.82%. The capacity was accordingly expected to be 0.23 milliequivalent/g. This stage was composed of three stages, as shown in Table II.

Kinetic study

This was based on Chatterjee's method²⁸ with the following general equation for the rate of the heterogeneous kinetics (V):

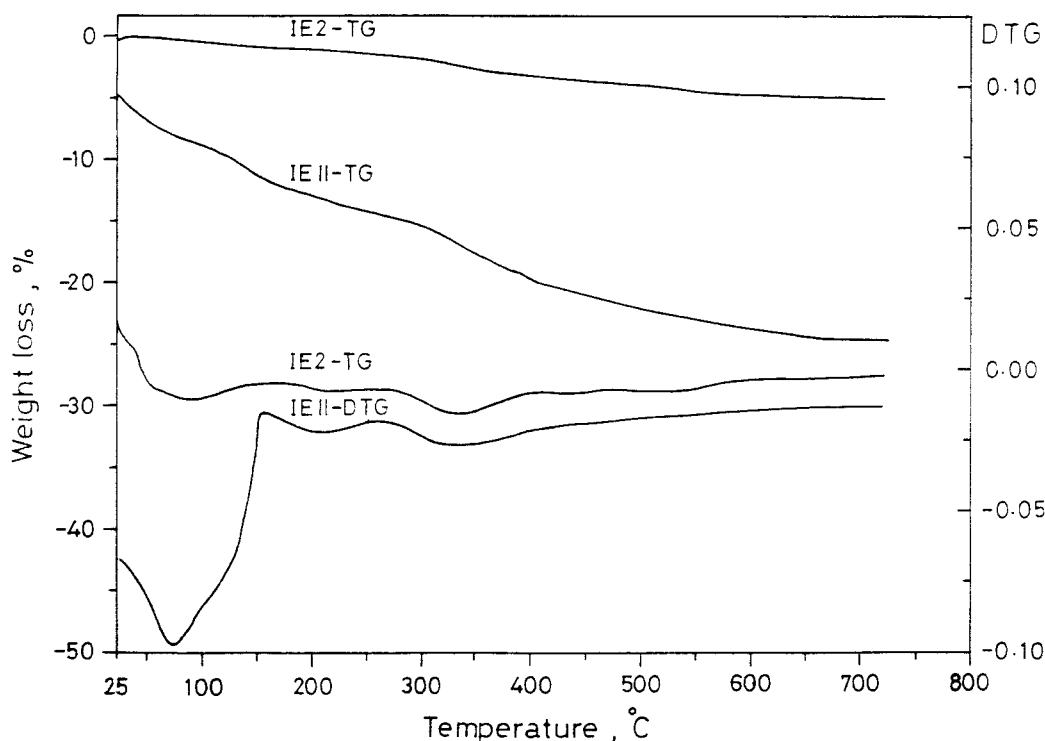


Figure 5 Thermogravimetric analysis of ion exchangers IE11 and IE2.

$$V = -dm/dt = km^n \quad (1)$$

where k , m , n , and t are the specific reaction rate constant, the active mass of the decomposing material (mg), the reaction order (1), and the time elapsed from the start of the experiment (min), respectively.

Substituting k from the Arrhenius equation into eq. (1) gives

$$\text{Log} V = \text{log} A - n \text{log} m - E_a/2.303RT \quad (2)$$

where A is the frequency factor and R is the gas constant. This equation gives the relationship between the reaction rate and temperature. The energy of activation (E_a) can be calculated from the slope S of the

straight line from the plot of $\text{log} V$ versus $1/T$, where $E_a = 2.303RS$.

The magnitude of E_a measured for a solid phase decomposition reaction has often been explained by the energy barrier in the limiting step, such as bond rupture, electron or proton transfer, or enthalpy of decomposition. The evaluated values of k and E_a are given in Table II. It is clear that the order of the decomposition reaction for all cases was unity. This indicates that the decomposition reaction followed the same mechanism.²⁹ The second stage in IE11 and the third in IE2 were suggested to be due to the liberation of the aromatic part of the substrate, as it had the highest E_a value and the aromatic part needed more energy to destroy the strong bonds C=N and C—Ph.

TABLE II
Analysis of the TG Curves of the Thermal Decomposition of IE11 and IE2

Stage	Range (°C)	Midpoint (°C)	Weight loss (%)	IE11				
				$k \times 10^3$ (s ⁻¹)	E_a (kJ mol ⁻¹)	ΔS^* (J K ⁻¹ mol ⁻¹)	ΔH^* (kJ mol ⁻¹)	$-\Delta G^*$ (kJ mol ⁻¹)
IE11								
First	78–152	115	6.1	1.33	9.93	172.00	6.68	60.09
Second	174–258	207.1	2.49	4.83	57.81	215.98	53.63	52.01
Third	258–421	310.7	10.84	0.84	15.72	168.72	10.58	92.78
Total					83.96	556.70	70.89	204.88
IE2								
First	71–128	92.3	0.75	4.26	27.37	197.81	24.28	48.01
Second	187–301	218.0	0.98	2.43	32.03	190.51	27.88	65.69
Third	301–372	333.0	1.30	2.97	57.16	203.09	52.01	71.09
Fourth	372–579	475.5	1.66	1.41	38.27	180.90	31.96	103.47
Total					159.83	77.31	136.13	288.26

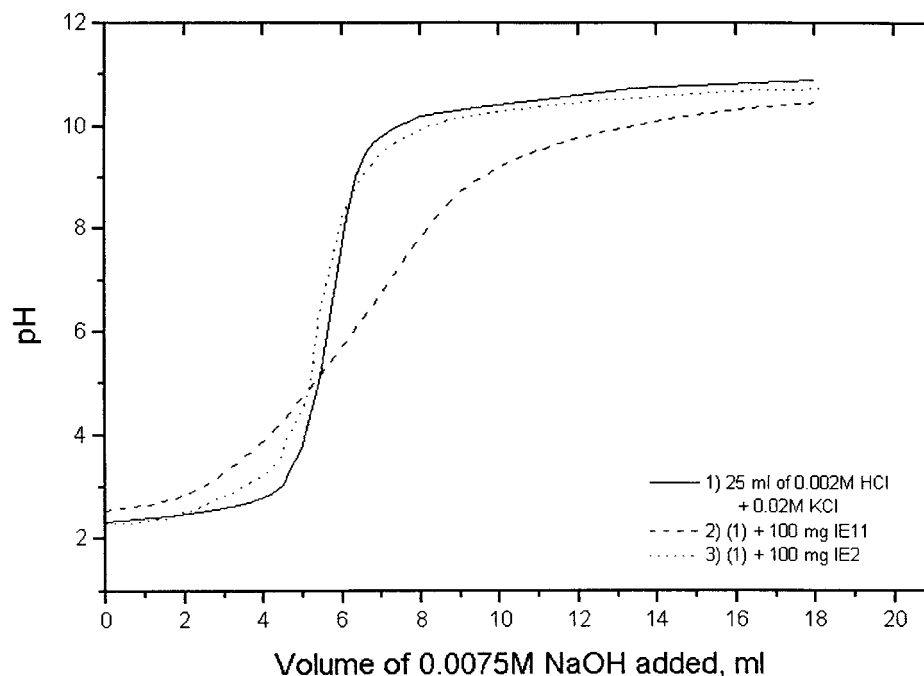


Figure 6 pH-metric titration curves of IE11 and IE2.

Thermodynamic parameter calculation

The thermodynamic parameters ΔH^* , ΔG^* , and ΔS^* for the thermal decomposition process were calculated with the values of the specific rate constant in each stage according to the rate theory and the Arrhenius equation.²⁹ The obtained values are summarized in Table II. According to this table, the values of $\Delta H^*_{\text{total}}$ and $\Delta S^*_{\text{total}}$ for all stages were positive, and this clearly means that the decomposition process was endothermic and was accompanied by an increase in the disorder of the decomposition products. It is clear also that IE2 had E_a and other thermodynamic parameters such as $\Delta H^*_{\text{total}}$, $\Delta G^*_{\text{total}}$, and $\Delta S^*_{\text{total}}$ higher than those of IE11 (Table II). This indicates that IE11 was more active than IE2 because of its high surface area.

pH-metric titration

Representative pH-metric titration curves of IE11 and IE2 with 0.0075M NaOH are shown in Figure 6. Both ion exchangers showed two inflection points. The values of $pK_1^H = 3.8$ and $pK_2^H = 9.7$ refer to the stepwise dissociation of two protons.³⁰ The first inflection point was due to proton gained from the HCl solution causing a retardation in the pH curve with respect to that of 0.002M HCl.

The protonation of the nitrogen atom was also confirmed by IR, ¹H-NMR, and mass spectrometry. The tendency of nitrogen-containing ion exchangers to form protonated species was mentioned previously for the chemically modified chloromethylated polystyrene-PAN ion exchanger³¹ and for silica-based ion exchangers.³²

The second inflection was suggested to be attributed to a deprotonation process through the phenolic OH group. The capacity calculated at the end of this process was found to be 0.44 and 0.059 milliequivalent/g for IE11 and IE2, respectively; this is the same order of those predicted from thermal analysis.

Capacity

The capacity measured for IE11 and IE2 with the amount of separated Cu(II) at pH 5.5 were 0.36 and 0.026 mmol of Cu/g, respectively. These values were lower than those found by the pH-metric method, and this may be attributed to the presence of some of the Schiff-base groups in tunnels and pores of the silica that could not be accessed by the Cu²⁺ ions, whereas it was accessible by H⁺ because of the large difference in size.

Generally, IE11 showed much higher capacity than IE2, and this agreed with the results of the thermogravimetric analysis. The obtained capacity of IE11 was relatively high in comparison with reported silica-based ion exchangers; MAF-8HQ has a capacity of 0.28 mmol of Cu/g,¹⁰ and silica grafted with 3-aminopropyltriethoxysilane^{33,34} or 3-mercaptopropyltrimethoxysilane³⁴ has a capacity of 0.032 mmol of Cu/g. This is an important indication of obtaining highly porous silica.

The distribution coefficient (K_d) and recovery (R) of the metal ions are calculated by the following equations:¹¹

$$K_d(\text{cm}^3/\text{g}) = C_{\text{IE11}}/C_{\text{sol}} \quad (3)$$

TABLE III
 k_d (cm³/g) and R (%) Values of Some Metal Ions
at Different pH Values

pH	Cd(II)		Cu(II)		Pb(II)	
	R	$\text{Log } k_d$	R	$\text{Log } k_d$	R	$\text{Log } k_d$
10.7	80.65	3.72	92.0	4.16	92.62	4.20
8.8	97.41	4.67	94.24	4.31	96.22	4.50
7.5	22.09	2.55	97.06	4.62	97.19	4.64
5.5	11.07	2.19	46.49	3.04	46.57	3.04

where C_{IE11} and C_{sol} are the concentrations of the metal ion in the ion exchanger matrix IE11 ($\mu\text{g/g}$) and that in the solution ($\mu\text{g/cm}^3$), and

$$R(\%) = k_d E_{\text{IE11}} \times 100 / (k_d W_{\text{IE11}} + V) \quad (4)$$

where W_{IE11} is the weight of the ion exchanger used and V is 25 cm³, which is the volume of the solution used.

The distribution of some metal ions [chosen to be Cd(II), Cu(II), and Pb(II)] between the solution and IE11 was evaluated with K_d and R values (Table III). They reflected the possibility of using IE11 in some analytical applications, such as preconcentration and separation.

CONCLUSIONS

IR, UV, ¹H-NMR, mass spectrometry, and thermal analysis confirmed the immobilization of *N*-propyl-salicylaldimine on controlled-pore silica. A larger porosity increased the capacity (C) of the ion exchanger. Also, thermogravimetric and differential thermogravimetric analysis data were used to study the kinetics of the thermal decomposition process of IE11.

IE11 acquired a capacity as high as that of known chelating ion exchangers ($C_{\text{IE11}} = 0.36$ mmol of Cu/g). $\text{Log } K_d$ values of IE11 toward some metal ions was within the range of 2.19–5.16, and this indicated the possibility of using it in some analytical applications.

References

- Lingane, J. J. *Electroanalytical Chemistry*, 2nd ed.; Interscience: New York, 1958.
- Olsen, S.; Pessenda, L. C. R.; Ruzicka, J.; Hansen, E. H. *Analyst* (London) 1983, 108, 905.
- Hiraide, M.; Yoshida, Y.; Mizuike, A. *Anal Chim Acta* 1976, 81, 185.
- Burba, P.; Willmer, P. G. *Fresenius Z Anal Chem* 1987, 321, 109.
- Kenawy, I. M.; Hafez, M. A. *Analisis* 1996, 24, 275.
- Kenawy, I. M. *Anal Sci* 1992, 8, 45.
- Kim, Y. S.; Zeitlin, H. *Anal Chim Acta* 1969, 46, 1.
- Orians, K.; Boyle, E. *Anal Chim Acta* 1993, 282, 63.
- Beinrohr, E.; Akrt, M.; Garaj, J.; Rapta, M. *Anal Chim Acta* 1990, 230, 163.
- Sohrin, Y.; Iwamoto, S.; Akiyama, S.; Fujita, T.; Kugii, T.; Obata, H.; Nakayama, E.; Goda, S.; Fujishima, Y.; Hasegawa, H.; Ueda, K.; Matsui, M. *Anal Chim Acta* 1998, 363, 11.
- Abdelaal, M.; Kenawy, I.; Hafez, M. *J Appl Polym Sci* 2000, 77, 3044.
- Izatt, R.; Bruening, R.; Bruening, M.; Tarbet, B.; Krakowiak, K.; Bradshaw, J.; Christensen, J. *Anal Chem* 1988, 60, 1825.
- Leyden, D. E.; Luttrell, G. H. *Anal Chem* 1975, 47, 1612.
- Seshadri, T.; Kettrup, A. *Fresenius Z Anal Chem* 1979, 296, 247.
- Konijnendijk, W. L. Ph.D. Thesis, Technological University Eindhoven, 1975.
- Fernandes, J.-C. B.; Neto, G.; Kubota, L. *Anal Chim Acta* 1978, 366, 11.
- Akman, S.; Ince, H.; Köklü, Ü. *Anal Sci* 1991, 7, 799.
- Griscom, D. In *Materials Science Research 12, Proceedings of the Conference on Boron in Glass and Glass Ceramics*, Alfred, New York, June 5–8, 1977; Bye, L.; Fréchette, V.; Kreidle, N., Eds.; Plenum: New York, 1978; p 75.
- Khalil, E.; Aouf, M. *Bull NRC (Egypt)* 1998, 23, 253.
- Ying, J.; Benziger, J. *J Am Ceram Soc* 1993, 76, 2561.
- Khalil, E.; Aouf, M. *Bull NRC (Egypt)* 1998, 23, 269.
- Smith, C. In *Materials Science Research 12, Proceedings of the Conference on Boron in Glass and Glass Ceramics*, Alfred, New York, June 5–8, 1977; Bye, L.; Fréchette, V.; Kreidle, N., Eds.; Plenum: New York, 1978; p 307.
- Konijnendijk, W.; Stevels, J. In *Materials Science Research 12, Proceedings of the Conference on Boron in Glass and Glass Ceramics*, Alfred, New York, June 5–8, 1977; Bye, L.; Fréchette, V.; Kreidle, N., Eds.; Plenum: New York, 1978; p 259.
- Parikah, V. M. *Absorption Spectroscopy of Organic Molecules*; Addison-Wesley: London, 1974.
- Looker, J. H.; Hanneman, W. *J Org Chem* 1962, 27, 381.
- Metzler, D. *J Am Chem Soc* 1957, 79, 485.
- Mcquate, R.; Leussing, D. *J Am Chem Soc* 1975, 97, 5117.
- Chatterjee, P. K. *J Polym Sci Part A-1*, 1968, 6, 3217.
- Emam, M. E. M.; Kenawy, I. M. M.; Hafez, M. A. *Thermochim Acta* 1995, 249, 169.
- Albert, A.; Serjeant, E. *The Determination of Ionization Constants*, 2nd ed.; Chapman & Hall: Edinburgh, Scotland, 1971; p 93.
- Kenawy, I.; Hafez, A. M.; Lashien, R. *Anal Sci* 2000, 16, 493.
- Mahmoud, M. *Anal Lett* 1996, 29, 1791.
- Ince, H.; Akman, S.; Köklü, U. *Fr J Anal Chem* 1992, 342, 560.
- Akman, S.; Ince, H.; Koklu, U. *J Anal At Abs Spectrom* 1992, 7, 187.